

# Enhanced CD1d phosphatidylserine presentation using a single-domain antibody promotes immunomodulatory CD1d-TIM-3 interactions

Roeland Lameris <sup>1</sup>, Adam Shahine,<sup>2</sup> Myrthe Veth,<sup>1</sup> Bart Westerman,<sup>3</sup> Dale I Godfrey,<sup>4</sup> David Lutje Hulsik,<sup>5</sup> Patricia Brouwer,<sup>5</sup> Jamie Rossjohn,<sup>2,6</sup> Tanja D de Gruijl,<sup>1</sup> Hans J van der Vliet<sup>1,5</sup>

**To cite:** Lameris R, Shahine A, Veth M, *et al.* Enhanced CD1d phosphatidylserine presentation using a single-domain antibody promotes immunomodulatory CD1d-TIM-3 interactions. *Journal for ImmunoTherapy of Cancer* 2023;**11**:e007631. doi:10.1136/jitc-2023-007631

► Additional supplemental material is published online only. To view, please visit the journal online (<http://dx.doi.org/10.1136/jitc-2023-007631>).

Accepted 05 November 2023

## ABSTRACT

**Background** CD1d is a monomorphic major histocompatibility complex class I-like molecule that presents lipid antigens to distinct T-cell subsets and can be expressed by various malignancies. Antibody-mediated targeting of CD1d on multiple myeloma cells was reported to induce apoptosis and could therefore constitute a novel therapeutic approach.

**Methods** To determine how a CD1d-specific single-domain antibody (VHH) enhances binding of the early apoptosis marker annexin V to CD1d<sup>+</sup> tumor cells we use in vitro cell-based assays and CRISPR-Cas9-mediated gene editing, and to determine the structure of the VHH1D17-CD1d(endogenous lipid) complex we use X-ray crystallography.

**Results** Anti-CD1d VHH1D17 strongly enhances annexin V binding to CD1d<sup>+</sup> tumor cells but this does not reflect induction of apoptosis. Instead, we show that VHH1D17 enhances presentation of phosphatidylserine (PS) in CD1d and that this is saposin dependent. The crystal structure of the VHH1D17-CD1d(endogenous lipid) complex demonstrates that VHH1D17 binds the A'-pocket of CD1d, leaving the lipid headgroup solvent exposed, and has an electro-negatively charged patch which could be involved in the enhanced PS presentation by CD1d. Presentation of PS in CD1d does not trigger phagocytosis but leads to greatly enhanced binding of T-cell immunoglobulin and mucin domain containing molecules (TIM)-1 to TIM-3, TIM-4 and induces TIM-3 signaling.

**Conclusion** Our findings reveal the existence of an immune modulatory CD1d(PS)-TIM axis with potentially unexpected implications for immune regulation in both physiological and pathological conditions.

## INTRODUCTION

CD1 molecules are major histocompatibility complex (MHC) class I-like molecules that, in contrast to MHC class I and II molecules, are monomorphic and present lipid-based antigens in their hydrophobic antigen-binding cleft.<sup>1,2</sup> Based on sequence homology, membrane CD1 molecules are divided in group 1 (CD1a, CD1b and CD1c)

## WHAT IS ALREADY KNOWN ON THIS TOPIC

- ⇒ Antibody-mediated targeting of CD1d on multiple myeloma cells was reported to induce annexin V binding, suggestive of apoptosis.
- ⇒ Externalization of phosphatidylserine (PS) in cells undergoing apoptosis has been recognized for its role in (cancer) immune tolerance via interaction with TIM-molecules.

## WHAT THIS STUDY ADDS

- ⇒ We show that CD1d-antibody ligation does not induce cell death but instead enhances CD1d-PS presentation.
- ⇒ CD1d-PS can interact with TIM-1, TIM-3, TIM-4, and enhances TIM-3 signaling, revealing the existence of an immune modulatory CD1d(PS)-TIM axis.
- ⇒ Our findings suggest that the role of CD1d goes beyond providing direct lipid antigen-dependent T cell receptor (TCR) stimulation but can also provide co-stimulatory/inhibitory signals via ligation of TIM-molecules expressed on various immune cells.

## HOW THIS STUDY MIGHT AFFECT RESEARCH, PRACTICE OR POLICY

- ⇒ Considering the role of TIM-3 as an immune checkpoint in autoimmunity and cancer, targeting the CD1d(PS)-TIM axis could have implications for immune regulation in both physiological and pathological conditions.

and group 2 (CD1d).<sup>1</sup> CD1d is preferentially expressed on both healthy and malignant cells of (myelo)monocytic origin (eg, monocytes, macrophages, dendritic cells and acute myeloid leukemia) and of the B cell lineage (eg, B cells, multiple myeloma (MM), chronic lymphocytic leukemia) but can also be found on several epithelial cell types and tumors (eg, intestinal epithelial cells, extravillous trophoblast, renal cell carcinoma).<sup>3-7</sup> On biosynthesis in the endoplasmic reticulum (ER), CD1d molecules travel the secretory



© Author(s) (or their employer(s)) 2023. Re-use permitted under CC BY-NC. No commercial re-use. See rights and permissions. Published by BMJ.

For numbered affiliations see end of article.

## Correspondence to

Professor Hans J van der Vliet; [jj.vandervliet@amsterdamumc.nl](mailto:jj.vandervliet@amsterdamumc.nl)

pathway to the plasma membrane for subsequent recycling between the plasma membrane and endosomal network which is mediated via their cytoplasmic tail.<sup>2</sup> Traveling these distinct cellular compartments, endogenous (eg, sphingolipids and phospholipids) and exogenous lipid antigens are continuously exchanged by help of lipid transfer proteins (LTP) for presentation to T cells on the cell surface.<sup>8</sup> These CD1d restricted T cells can be divided in two groups; type 1 natural killer T (NKT) cells which express a semi-invariant TCR and strongly react to the lipid antigen  $\alpha$ -galactosylceramide ( $\alpha$ -GalCer), and diverse type NKT cells which express a broad TCR repertoire and respond to various (partly unknown) lipid antigens.<sup>3,9</sup> Whereas the former has been extensively studied and recognized for its strong inherent antitumor activity, the latter likely represents a more sizeable population in human and appears to have a more immunoregulatory role.<sup>3,10</sup>

Besides affecting CD1d-TCR interactions, it was reported that CD1d-antibody ligation, similar to CD1b-antibody and CD1c-antibody (but not CD1a-antibody) ligation, could trigger downstream receptor signaling and activation.<sup>11–13</sup> Antibody ligation of CD1d induced monocyte differentiation and triggered apoptosis (reflected by enhanced annexin V binding) of MM cells.<sup>11,12</sup> Induction of apoptosis was caspase independent but required the cytoplasmic tail of CD1d.<sup>12</sup> From a generated panel of CD1d-specific single-domain antibodies (VHH) we previously identified one specific clone (VHH1D17) that similarly enhanced annexin V binding,<sup>14</sup> suggestive of early apoptosis, on binding to CD1d<sup>+</sup> malignant hematologic cells. Since induction of early apoptosis could synergize with established anti-MM therapies and sensitize MM cells for macrophage phagocytosis, we here set out to explore the mechanism of action of VHH1D17 and how this could be exploited in CD1d-expressing malignancies. By using a structural and functional approach, we found that the VHH1D17-induced enhancement of annexin V binding does not reflect cell-death induction but rather increased presentation of anionic phospholipid antigens in the antigen-binding groove of CD1d, and that presentation of these anionic phospholipids allowed for interaction with immunomodulatory TIM-molecules.

## METHODS

Flow cytometry and antibodies, cells lines, generation and binding of CD1d-specific VHHs, stimulation of TCR-expressing SKW-3 cells, crystallization and structure determination, monocyte-derived macrophages and stimulation of CD16-expressing NK-92 cells are described in the online supplemental methods.

### Annexin V binding and viability assessment

The effect of VHH1D17 on annexin V binding and cell viability was assessed by flow cytometry.  $1 \times 10^5$  C1R.WT, C1R.CD1d cells, MM.1s.WT, MM.1s.CD1d cells or HeLa.CD1d cells were incubated with indicated concentrations

of anti-CD1d VHH (VHH1D17 (wild-type (WT) or mutant), VHH1D5, VHH1D control) or monoclonal antibody (mAb) anti-CD1d 51.1 ( $5 \mu\text{g mL}^{-1}$ , BioLegend cat# 350304) for up to 72 hours. After incubation cells were washed in annexin V binding buffer and briefly incubated with annexin V-fluorescein isothiocyanate (FITC) and propidium iodide (PI) or 7-aminoactinomycin D (7-AAD), for subsequent flow cytometry analysis. Relative viability was calculated by dividing the percentage living (PI/7-AAD<sup>-</sup>) (condition) by percentage living (control) cells multiplied by 100. Alternatively, living cells (7-AAD<sup>-</sup>) were quantified using flow cytometric counting beads, and the relative percentage of living cells (7-AAD<sup>-</sup>) was calculated by dividing the absolute cell number (condition) by absolute cell number (control) multiplied by 100. Cell expansion was determined after 96 hours culture by manual counting (trypan blue exclusion). Median fluorescence index (MFI) was calculated by dividing median fluorescence (MF) (condition) by MF (control).

To determine whether annexin V was bound to lipids loaded in CD1d, the type 1 NKT cell blocking anti-CD1d VHH1D22<sup>14,15</sup> (500 nM) was added to the cell culture during or after 24 hours incubation with VHH1D17. In conditions where VHH1D22 was added after incubation, it was done so at 4°C and 1 hour prior to analyses.

### Inhibition of CD1d lipid loading

Lipid loading of CD1d in the ER was inhibited by the microsomal triglyceride transfer protein (MTP) inhibitor lomitapide (Sigma cat #SML1385).  $1 \times 10^5$  C1R.CD1d cells were incubated with 1 nM lomitapide (higher concentrations induced significant cell death) or dimethyl sulfoxide (DMSO) control (0.005%)  $\pm$  VHH1D17 (100 nM) for 24 hours after which cells were analyzed as described above.

To inhibit saposin-mediated lipid loading of CD1d in the endosomal compartment, the prosaposin (PSAP) gene was knocked down using short hairpin RNA (shRNA) plasmids (sureSilencing, Qiagen cat #336312).  $2 \times 10^5$  C1R.CD1d cells were transfected with PSAP shRNA-plasmid and control shRNA-plasmid (ie, scrambled artificial sequence) using Attractene transfection reagent (Qiagen cat #301005) according to the manufacturer's instructions, followed by positive selection with hygromycin B ( $200 \mu\text{g mL}^{-1}$ ). Knockdown was confirmed by intracellular staining for PSAP and subsequent flow cytometry analysis. The effect of VHH1D17 on annexin V binding was analyzed as described above.

By using CRISPR-mediated genome editing, a PSAP KO C1R.CD1d cell line (C1R.CD1d.KO/PSAP) was established essentially as described<sup>16</sup> and online supplemental methods. The effect of VHH1D17 on annexin V binding was analyzed as described above.

### Bavituximab and TIM binding

The effect of VHH1D17 on rhTIM-1, rhTIM-3 and rhTIM-4, and bavituximab binding was assessed by flow cytometry.  $1 \times 10^5$  C1R.CD1d cells and C1R.CD1d.PSAP/

KO cells were incubated ± anti-CD1d VHH1D17 for 24 hours. rhTIM-1, rhTIM-3 to rhTIM-4Fc and bavituximab were pre-incubated with anti-Fc-PE for 20 min at room temperature, blocked with normal human serum (Merck Millipore cat# S1) for 20 min and subsequently used to stain C1R.CD1d cells suspended in annexin V buffer, for subsequent flow cytometry analysis. MFI was calculated by dividing MF (condition) by MF (control).

### TIM-3 reporter cell assay

The effect of VHH1D17 on TIM-3 signaling was assessed using the TIM-3 bioassay (Thaw and Use kit, Promega cat #JA2211).  $5 \times 10^4$  C1R.CD1d cells and C1R.CD1d.PSAP/KO cells were incubated ± anti-CD1d control or anti-CD1d VHH1D17 for 24 hours prior to co-culture with TIM-3 effector cells (that express human TIM-3 and TCR activation driven NanoLuc luciferase reporter), for an additional 20 hours followed by the addition of Bio-Glo-NL luciferase assay reagent. Bioluminescence was quantitated with a luminometer, according to the manufacturer's instructions.

### Statistical analysis

For in vitro experiments each n represents an independent experiment. No statistical method was used to predetermine sample size for the in vitro experiments. No data were excluded from the analyses. The experiments were not randomized and the investigators were not blinded to allocation during the experiments and outcome assessment. For data with one variable and two groups, a two-tailed paired/unpaired t-test was used to calculate the p value. For data with one variable and multiple groups, a mixed effect analysis or a one-way analysis of variance (ANOVA) with Tukey's multiple comparisons test to calculate the multiplicity-adjusted p value was used. For data with two variables, a two-way ANOVA with either Tukey's or Šídák's multiple comparisons test to calculate the multiplicity-adjusted p value was used. Dose-response curves, half maximal effective concentration ( $EC_{50}$ ) was calculated using non-linear regression (agonist vs response). Statistical details can be found in the figure legend. Statistical analysis was performed using Prism V.9.1.0 (GraphPad Software).

## RESULTS

### VHH1D17 enhances annexin V binding to CD1d expressing tumor cells but does not induce apoptosis

A panel of CD1d-specific VHHs was generated via immunization of *Lama glama*, phage library construction, and selection of specific clones.<sup>14</sup> Functional evaluation of these CD1d-specific VHHs identified anti-CD1d VHH1D17 to have the ability, like the anti-CD1d mAb clones 42.1 and 51.1,<sup>12</sup> to enhance annexin V binding to CD1d<sup>+</sup> tumor cells.<sup>14</sup> Annexin V specifically binds anionic phospholipids (eg, phosphatidylserine (PS)) in the presence of  $Ca^{2+}$  and can be used to measure PS on the outer leaflet of the plasma membrane as a marker of (early)

apoptosis.<sup>17</sup> VHH1D17 consistently enhanced annexin V binding to the whole population of CD1d transfected lymphoblastic C1R cells and MM.1s cells (figure 1A, B, online supplemental figure S1A). In contrast, enhanced annexin V binding induced by an anti-CD1d monoclonal antibody (clone 51.1) was only observed for a minor population of CD1d transfected C1R cells and not for the CD1d transfected MM.1s cells (figure 1A). Neither VHH1D17 nor CD1d mAb 51.1 were able to enhance annexin V binding to CD1d transfected HeLa adenocarcinoma cells (figure 1A, online supplemental figure S1A), known to differ in trafficking of CD1d.<sup>18 19</sup> We next explored the effect of VHH1D17 dose and duration of exposure on the induction of annexin V binding on CD1d transfected and WT C1R and MM.1s cells. Annexin V binding on exposure to VHH1D17 was CD1d and dose dependent ( $EC_{50}$  of 2.8 nM) and plateaued once established (figure 1B, online supplemental figure S1B).

As increased annexin V binding can be a sign of early apoptosis, we evaluated the viability of CD1d<sup>+</sup> C1R and MM.1s cells during culture and while we found exposure to VHH1D17 to result in a significantly lower (~10%) percentage of viable (PI<sup>-</sup>) cells in CD1d<sup>+</sup> MM.1s cells, C1R.CD1d or HeLa.CD1d viability was not affected (figure 1C, online supplemental figure S1C). Of note, also in CD1d<sup>+</sup> MM.1s cells this minor reduction in viability did not increase beyond 24 hours and was not accompanied by an actual reduction in the absolute number of living cells (figure 1C, D, online supplemental figure S1D). Anti-CD1d mAb clone 51.1 had no effect on relative viability or absolute number of living cells (online supplemental figure S1C, D). Of interest, the enhancement in annexin V binding induced by VHH1D17 was clearly of lower intensity compared with that observed in dead cells (ie, cells double positive for annexin V and a nuclear dye (PI, 7-AAD) (online supplemental figure S1E, F)). Collectively, these data showed that VHH1D17 enhanced annexin V binding to CD1d<sup>+</sup> C1R and MM cells but that this does not reflect (early) cell death.

### VHH1D17 enhances saposin-dependent presentation of anionic phospholipids in CD1d

In healthy cells, lipid transporters shuttle PS to the inner leaflet of the plasma membrane and thereby maintain a highly asymmetrical distribution which is lost on (early) apoptosis. PS externalization can however also occur in conditions not related to cell death, for example, in stressed and activated immune cells.<sup>20 21</sup> Moreover, it has also been shown that a range of (anionic) phospholipids, which includes PS, can be presented by CD1d.<sup>22</sup> Therefore, we evaluated whether the VHH1D17 enhanced annexin V binding to CD1d<sup>+</sup> tumor cells could be due to increased anionic phospholipid antigen presentation in CD1d. First we investigated if binding of annexin V could be blocked by the CD1d specific VHH1D22 that binds over the side of the F'-pocket of CD1d and thereby abrogates type 1 NKT-cell activation.<sup>15</sup> VHH1D22, when added 1 hour prior to the addition of annexin V during

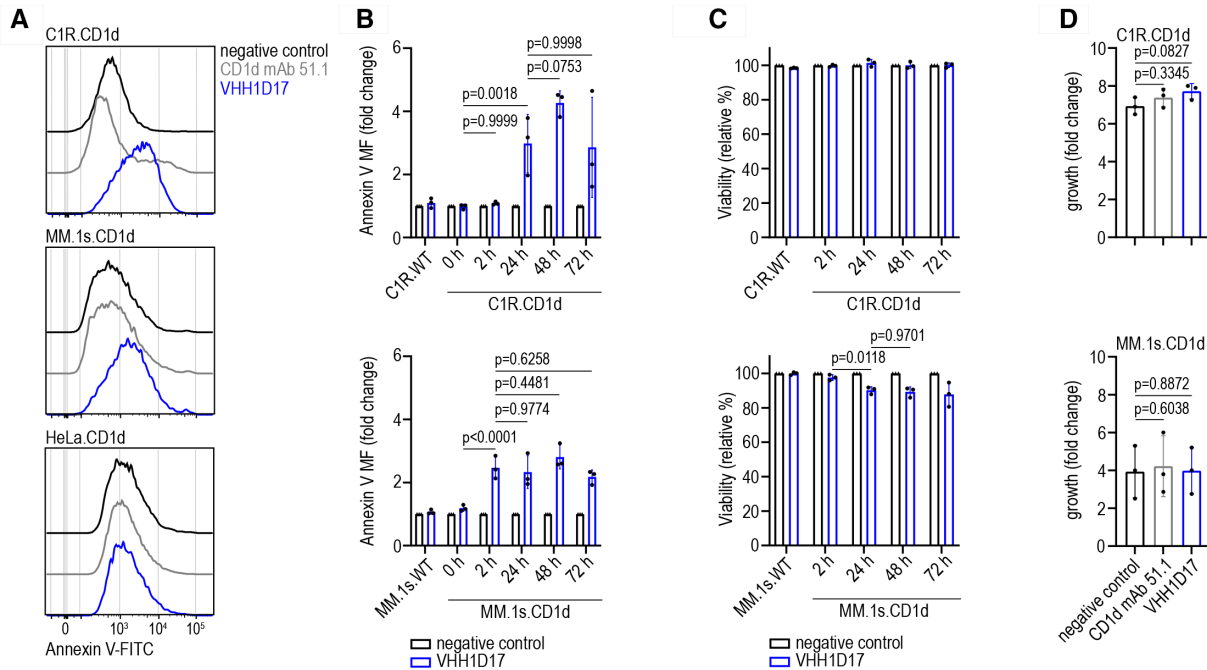


**Figure 1** CD1d-specific VHH1D17 enhances non-apoptotic annexin V binding. (A) Histograms depicting binding of annexin V to C1R.CD1d cells after 24 hours culture plus negative control (black), anti-CD1d mAb (clone 51.1, ~33 nM, gray) or VHH1D17 (100 nM, blue). Data are representative of three independent experiments. (B) Fold change in annexin V binding to WT or CD1d transduced C1R or MM.1s cells after 24 hours (WT) or 0, 2, 24, 48 or 72 hours culture plus negative control or VHH1D17 (100 nM) ( $n=3$  independent experiments). (C) Relative viability of WT or CD1d transduced C1R or MM.1s cells after 24 hours (WT) or 0, 2, 24, 48 or 72 hours culture plus negative control or VHH1D17 (100 nM) ( $n=3$  independent experiments). (D) Growth of C1R.CD1d and MM.1s.CD1d cells after 4 days culture with negative control, anti-CD1d mAb (clone 51.1, ~33 nM) or VHH1D17 (100 nM) ( $n=3$  independent experiments). The bars indicate the mean  $\pm$  SD. (B,C) Two-way ANOVA with Tukey multiple comparisons test. (D,) One-way ANOVA with Tukey multiple comparisons test. ANOVA, analysis of variance; mAb, monoclonal antibody; MF, median fluorescence; WT, wild-type.

analysis (at 4°C), resulted in a clear reduction in the capacity of annexin V to bind to CD1d<sup>+</sup> C1R cells that had been cultured in the presence of VHH1D17. Furthermore, the increase in annexin V binding to CD1d<sup>+</sup> C1R cells induced by VHH1D17 was completely lost when VHH1D22 was added at the start of the 24 hours culture (figure 2A, online supplemental figure S1G), suggesting that the observed increase in annexin V binding resulted from an increased interaction with CD1d-anionic phospholipid complexes. To determine whether VHH1D17 indeed enhanced the presentation of anionic phospholipids in CD1d, we interfered with two different LTPs known to be involved in lipid loading of CD1d. Inhibition of microsomal triglyceride transfer protein (MTP), an ER located LTP,<sup>8</sup> using lomitapide did not impact the VHH1D17 induced increase in annexin V binding (figure 2B). In contrast, shRNA-mediated knockdown (KD) of PSAP, the precursor of saposins A–D which facilitate loading of endogenous and exogenous lipids in the endosomal/lysosomal compartment after recycling of CD1d from the cell membrane,<sup>8</sup> clearly reduced and delayed the effect of VHH1D17 on annexin V binding to CD1d<sup>+</sup> C1R cells (figure 2C, online supplemental figure S1H) shows that PSAP KD as expected reduced PSAP levels but did not affect CD1d expression). To further confirm saposin dependence of this process, we generated

CRISPR-Cas9-mediated PSAP knockout (KO) CD1d<sup>+</sup> C1R cells (C1R.CD1d KO/PSAP). As shown, KO/PSAP cells were completely deficient of PSAP protein while CD1d expression was not affected (figure 2D, online supplemental figure S1I, J), and resulted in a complete ablation of the capacity of VHH1D17 to increase annexin V binding (figure 2E, online supplemental figure S1K).

These data thus demonstrated that the enhanced binding of annexin V to CD1d<sup>+</sup> tumor cells exposed to VHH1D17 resulted from increased, saposin dependent, anionic phospholipid antigen loading of CD1d in the endosomal/lysosomal compartment.

### Molecular basis of the VHH1D17-CD1d interaction

To analyze the molecular basis of the interaction between VHH1D17 and CD1d and how this could impact lipid loading, we determined the crystal structure of the VHH1D17-CD1d (endogenous lipid) complex at 2.3 Å and compared it to the VHH1D5-CD1d ( $\alpha$ -GalCer) crystal structure (Protein Data Bank (PDB) code 6V7Y)<sup>15</sup> as this VHH has a high sequence homology to VHH1D17 but does not enhance annexin V binding (figure 3A, online supplemental figure S2A, online supplemental tables S1 and S2). The electron density for the endogenous lipid bound in CD1d matched a sphingomyelin C24:1. The crystal structure

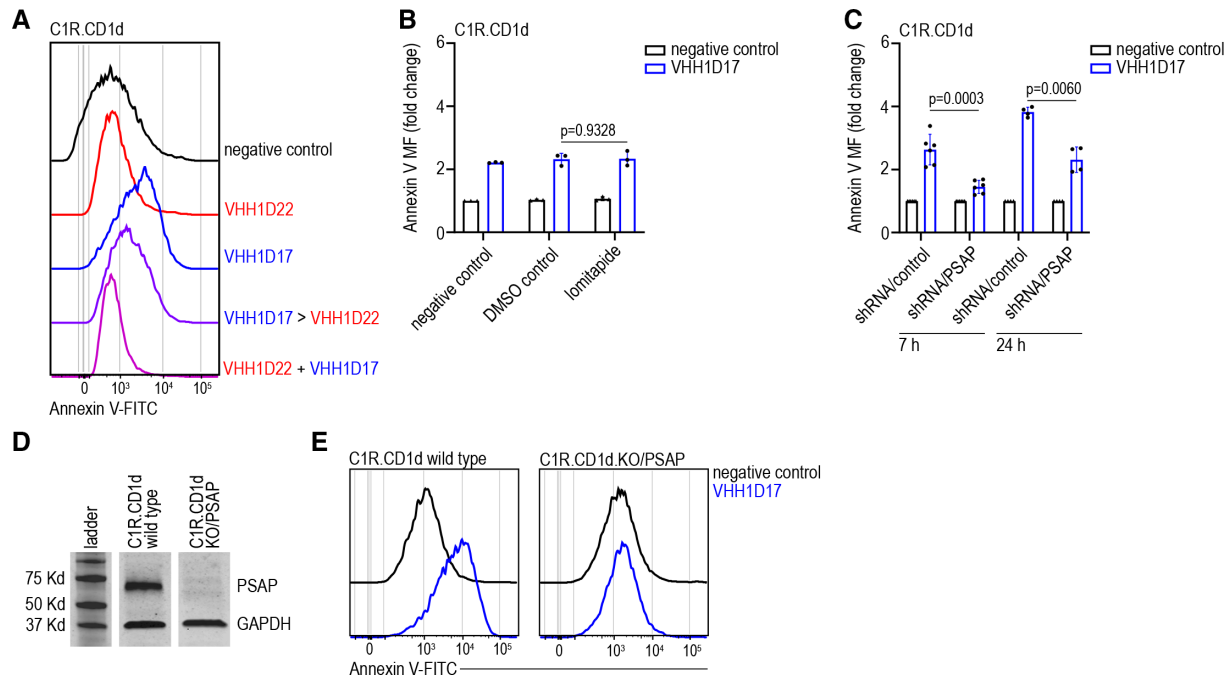


**Figure 2** VHH1D17 enhances saposin dependent presentation of anionic phospholipids by CD1d. (A) Histograms depicting the binding of annexin V to C1R.CD1d cells after 24 hours culture plus negative control (black), anti-CD1d VHH1D22 (100 nM) (red), VHH1D17 (100 nM) (blue) or a combination thereof. VHH1D17>VHH1D22; VHH1D22 (500 nM) was added 1 hour before readout at 4°C. Data are representative of three independent experiments. (B) Fold change in annexin V binding to CD1d transduced C1R cells after 24 hours culture plus negative control, DMSO control (0.005%), lomitapide (1 nM), VHH1D17 (100 nM) or a combination thereof (n=3 independent experiments) (C) Fold change in annexin V binding to shRNA control or shRNA saposin (PSAP) transfected C1R.CD1d cells after 7 or 24 hours culture plus negative control or VHH1D17 (100 nM) (n=6 (7 hours), n=4 (24 hours) independent experiments). (D) Western blot analyses of PSAP in whole cell lysates of C1R.CD1d and C1R.CD1d KO for PSAP (KO/PSAP). (E) Histograms depicting binding of annexin V to C1R.CD1d and C1R.CD1d.KO/PSAP after 24 hours culture plus negative control or VHH1D17 (100 nM). Data are representative of three independent experiments. The bars indicate the mean±SD. (B, C) Two-way ANOVA with Tukey (B) or Šidák (C) multiple comparisons test. ANOVA, analysis of variance; DMSO, dimethyl sulfoxide; MF, median fluorescence; shRNA, short hairpin RNA.

of VHH1D17-CD1d(sphingomyelin) showed binding of VHH1D17 to the A'-pocket of CD1d by a network of van der Waals and hydrogen bond interactions that were highly similar to binding of VHH1D5 to CD1d (figure 3A). On ligation of VHH1D17 to CD1d the total buried surface area (BSA) was 1790 Å<sup>2</sup>, with the CDR3 loop mediating the predominant interactions with both α-helices of CD1d (71% BSA) relative to the interaction provided by the CDR1 and CDR2 loops (11% and 18% BSA, respectively), which both bound the α1-helix of CD1d (figure 3B, online supplemental table S3). In comparison, on CD1d ligation VHH1D5 had a total BSA of 1850 Å<sup>2</sup>, with the CDR3 loop spanning both α-helices of CD1d and mediating the predominant interaction (74% BSA) relative to the interaction provided by the CDR1 and CDR2 loops (13% BSA each).<sup>15</sup>

Alanine-substitution mutant C1R.GFP.CD1d cell lines confirmed the prominent role of the CDR3 loop of VHH1D17 by showing that substitution of the CD1d residue W160, which extensively interacts with the CDR3 loop, abolished binding of VHH1D17 (online supplemental figure S2B). While the CDR3 loop of VHH1D17 extended toward the F'-portal and formed

a hydrogen bond (R115) with the phosphate moiety (present in all phospholipids) of the presented sphingomyelin, the headgroup remained solvent exposed (figure 3A, B, online supplemental table S3). This indicates that VHH1D17 is not expected to block the lipid headgroup of (phospho)lipids from interacting with annexin V. In support, VHH1D17 also did not interfere with type 1 NKT cell activation when α-GalCer was loaded in CD1d suggesting that the glycosyl head group, which is important for specific recognition by the type 1 NKT TCR,<sup>23</sup> remained exposed (online supplemental figure S2C).

When further comparing the VHH1D5 and VHH1D17 structures, we observed a tight overlay with a core root mean square deviation of 0.7 Å, indicating highly similar folding (online supplemental figure S2D). A minor difference was observed in the CDR2 loop positions, whereby the D55-G55 substitution in VHH1D17 decreased CDR2-CD1d interactions compared with VHH1D5 (online supplemental tables S1 and S3). A likely more important difference between VHH1D5 and VHH1D17 is related to conformational differences in CDR3 positioning; specifically remodeling of R109. For VHH1D17, the bulky

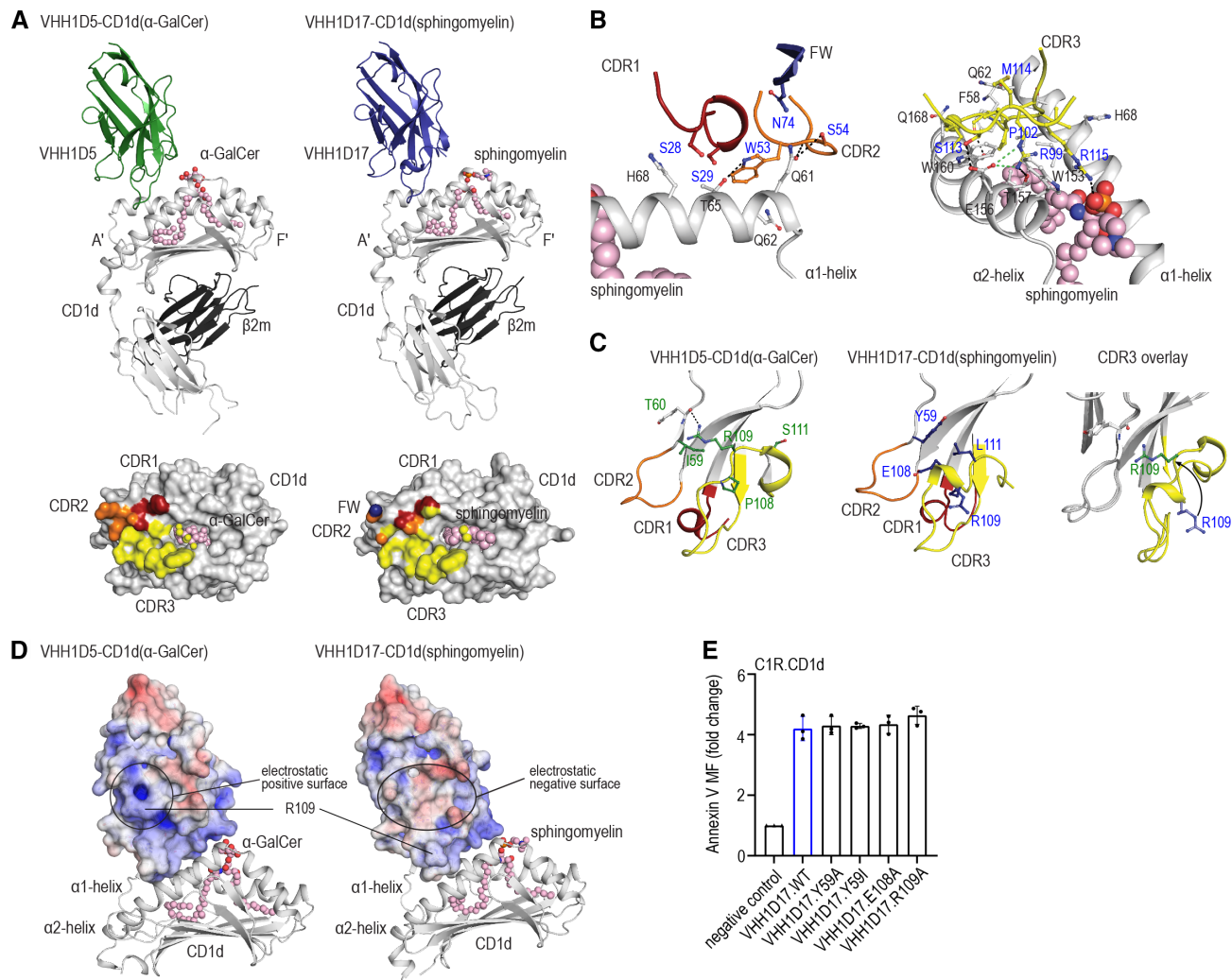


**Figure 3** VHH1D17 docks over the A'-pocket of CD1d. (A) Crystal structures of VHH1D5-CD1d( $\alpha$ -GalCer) (PDB accession code 6V7Y)<sup>15</sup> and VHH1D17-CD1d(sphingomyelin). Top: overview of each structure. Bottom: footprint of the VHH CDR regions on the CD1d(lipid) molecular surface. CD1d (gray),  $\beta$ 2M (black), VHH1D5 (green) and VHH1D17 (blue) are represented as ribbons (top) or CDR1 (red), CDR2 (orange), CDR3 (yellow) and framework (FW, blue) of VHH1D5 and VHH1D17 as molecular surface (bottom), with lipids (pink) represented as spheres. (B) Enlarged view of VHH1D17 CDR1, CDR2, CDR3 loop and FW interactions with CD1d(sphingomyelin). The residues involved in contacts are represented as sticks, with the hydrogen bonds and salt bridges represented as black and green dashed lines, respectively. Nitrogen, oxygen and sulfate are colored in blue, red and yellow, respectively. VHH1D17 residues are labeled in blue and CD1d residues in black. (C) Position of R109 on VHH1D5 compared with VHH1D17. VHH1D5 residues are labeled green, other residues and bonds are colored and depicted as stated previously. (D) Electrostatic surface potential of VHH1D5 and VHH1D17 bound to CD1d(lipid). The potential contours are shown on a scale from +5.0 (positive charge, blue) to  $-5.0 \text{ k}_B\text{T e}^{-1}$  (negative charge, red); white indicates a value close to  $0 \text{ k}_B\text{T e}^{-1}$  (neutral charge). (E) Fold change in annexin V binding to C1R.CD1d cells after 24 hours culture plus negative control or anti-CD1d VHH1D17 (100 nM, WT or single amino acid mutants) ( $n=3$  independent experiments). The bars indicate the mean  $\pm$  SD. WT, wild-type;  $\alpha$ -GalCer,  $\alpha$ -galactosylceramide.

side chain of Y59 caused a conformational change in the CDR3 region, pushing R109 towards the solvent (facing, but not contacting CD1d) (figure 3C). Whereas for VHH1D5, the smaller I59 residue and the P108, which likely prevented  $\alpha$ -helical formation due to steric hindrance, allowed R109 to flip towards the core of the VHH and form a hydrogen bond with the backbone of Y60 allowing the CDR3 region to curl upwards (figure 3C). This difference altered the surface architecture and electrostatics of the VHHs; where VHH1D5 had an electrostatically

positive surface, VHH1D17 had a (larger) slightly electrostatically negative surface (figure 3D), which is likely maintained (based on calculated electrostatic surface potentials using the PDB2PQR web server<sup>24</sup>) at a pH of 5 (online supplemental figure S2E) that is commonly encountered within the endosomal/lysosomal compartment.<sup>25</sup> Furthermore, binding of VHH1D17 to CD1d was not affected at this pH and was only reduced at pH 4.0, possibly due to heavily compromised cell viability (online supplemental figure S2F). Single alanine substitution mutations of

the amino-acids discordant between VHH1D5 and VHH1D17 as well as the Y59I substitution (presumed to be involved in positioning of the CDR3 region) in VHH1D17 did not reduce the ability of VHH1D17 to enhance annexin V binding (figure 3E, online supplemental figure S2G), suggesting that multiple dissimilar amino acids (likely Y59 and E108) are involved and required for allowing VHH1D17 to enhance annexin V binding to CD1d.

Collectively, these data demonstrate that VHH1D17 binds to the A'-pocket of CD1d and that VHH1D17 has an electro-negatively charged patch that is not present in VHH1D5, which could be involved in its ability to enhance anionic lipid presentation by CD1d.

### VHH1D17-enhanced CD1d-anionic phospholipid antigen presentation does not enhance efferocytosis but enhances binding to bavituximab and facilitates CD1d<sup>+</sup> tumor cells to interact with immunoregulatory TIM-molecules

Exposure of the anionic phospholipid PS on the outer membrane leaflet can have a strong immune modulatory function via multiple receptors, including TIM-molecules, and serve as an "eat-me" signal for efferocytosis by macrophages.<sup>20-26</sup> By using monocyte-derived (mo) Macrophages we showed that the VHH1D17-mediated

enhancement of anionic phospholipid presentation by CD1d does not result in increased efferocytosis whereas CD1d<sup>+</sup> MM cells pretreated with bortezomib, that triggers actual cell death (ie, an increase in 7-AAD<sup>+</sup> cells, (online supplemental figure S3A), were engulfed (figure 4A, online supplemental figure S3B). No such effect of bortezomib was observed at 4°C (online supplemental figure S3C), indicating efferocytosis and not simple binding interaction which would also occur at low temperatures.

Since PS exposure on tumor cells serves as an immunosuppressive signal, PS blocking antibodies may restore antitumor immunity.<sup>20</sup> One such antibody is bavituximab which binds to PS in complex with  $\beta$ 2-glycoprotein 1 (GP1) and can trigger Fc $\gamma$ -receptor mediated antibody-dependent cellular cytotoxicity (ADCC).<sup>27</sup> We therefore assessed whether VHH1D17 could impact bavituximab binding to tumor cells and thereby enhance bavituximab induced ADCC. Binding of bavituximab to CD1d<sup>+</sup> C1R cells was indeed significantly enhanced following culture with VHH1D17 (figure 4B, online supplemental figure S3D). However, VHH1D17 did not increase bavituximab-mediated degranulation by the NK cell line NK-92 transfected with Fc $\gamma$  receptor III (CD16) co-cultured with CD1d<sup>+</sup> C1R cells (online supplemental figure S3E).

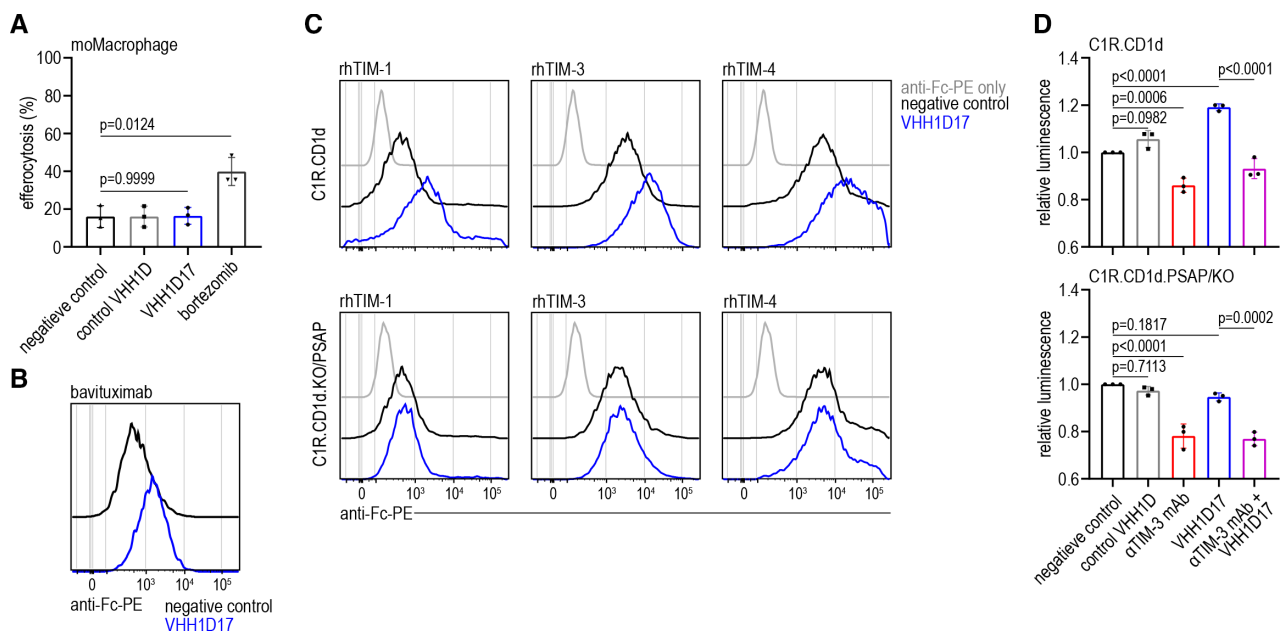


**Figure 4** VHH1D17 enhanced presentation of anionic phospholipids by CD1d results in increased binding to bavituximab and TIM-molecules and triggering of TIM-3 but not phagocytosis. (A) Phagocytosis (%) of CFSE labeled MM.1s.CD1d cells, pre-incubated for 24 hours with negative control, control VHH1D (100 nM), VHH1D17 (100 nM) or bortezomib (3 nM), by monocyte derived (mo)Macrophages after 4 hours coculture at 37°C (n=3 independent experiments). (B) Histograms depicting binding of bavituximab to C1R.CD1d cells after 24 hours culture plus negative control (black) or VHH1D17 (50 nM, blue), detected by anti-Fc-PE. Data are representative of three independent experiments. (C) Histograms depicting binding of recombinant human T-cell immunoglobulin and mucin domain containing protein (rhTIM)-1 to rhTIM-3 and rhTIM-4 to C1R.CD1d (WT or KO/PSAP) cells after 24 hours culture plus negative control (black) or VHH1D17 (100 nM, blue), detected by anti-Fc-PE. Data are representative of three independent experiments. (D) Relative bioluminescence of Tim-3 reporter cells after 20 hours co-culture with C1R.CD1d (WT or KO/PSAP) cells, pre-incubated for 24 hours with negative control, control VHH1D (100 nM) or VHH1D17 (100 nM), and  $\pm$ antiTIM mAb (10  $\mu$ g ml<sup>-1</sup>) (a triplicate is shown). The bars indicate the mean  $\pm$ SD. (A, D) One-way ANOVA with Tukey multiple comparisons test. ANOVA, analysis of variance; CFSE, carboxyfluorescein succinimidyl ester; KO, knockout; PSAP, prosaposin; WT, wild-type.

Bavituximab-induced degranulation of CD16 transfected NK-92 cells was already high in the absence of VHH1D17 and equivalent to that triggered by the anti-CD20 therapeutic antibody rituximab. Therefore, it is likely that (baseline) levels of PS exposed by C1R.CD1d cells co-cultured with NK92.CD16 cells were already sufficient to maximize degranulation.

We then studied whether VHH1D17 could enhance TIM-1, TIM-3, TIM-4 interactions. Analogous to enhanced annexin V binding, we observed a clear enhancement of binding of recombinant human (rh)TIM-1, TIM-3, TIM-4 to CD1d expressing C1R cells (figure 4C, online supplemental figure S3F) but not to the KO/PSAP CD1d expressing C1R cells (figure 4C, online supplemental figure S3F). Using a TIM-3 bioluminescence reporter cell-based assay we then investigated whether the VHH1D17-enhanced PS presentation by CD1d could promote TIM-3 signaling. Indeed, a clear increase in bioluminescence was observed on co-culture of TIM-3 reporter cells and VHH1D17 (but not control CD1d VHH) exposed C1R.CD1d cells, and this effect could be blocked by a neutralizing anti-TIM-3 mAb (figure 4D). Importantly, the capacity of VHH1D17 to increase TIM-3 signaling was completely abolished when using the KO/PSAP CD1d expressing C1R cells.

Overall, these data demonstrate that the VHH1D17-enhanced PS presentation by CD1d does not facilitate efferocytosis of CD1d<sup>+</sup> tumor cells, but does allow enhanced binding of PS-specific therapeutic antibodies to CD1d<sup>+</sup> tumor cells and interactions between CD1d<sup>+</sup> tumor cells and immunomodulatory TIM-molecules, including the widely expressed immune checkpoint TIM-3.

## DISCUSSION

In this study, we demonstrate that ligation of CD1d by anti-CD1d VHH1D17 enhances saposin-dependent presentation of anionic phospholipids by CD1d which can subsequently trigger TIM-3 signaling on immune effector cells. VHH1D17 bound over the A'-pocket of CD1d allowing the anionic phospholipid head-group present in CD1d to interact with annexin V as well as the PS-β2-GPI complex specific therapeutic antibody bavituximab, and the immune modulatory molecules TIM-1, TIM-3 and TIM-4.

In contrast to a previous report, that described caspase-activation-independent cell death on CD1d ligation by mAbs (clone 42.1 and 51.1),<sup>12</sup> our study demonstrated that enhanced annexin V binding by VHH1D17 and anti-CD1d mAb (clone 51.1) was not due to cell death. Observed discrepancies may be due to differences in the definition of cell death. Specifically, in the paper of Spanoudakis *et al*,<sup>12</sup> cell death was defined as an increase in annexin V binding or mitochondrial membrane potential loss, which are indeed associated with early apoptosis but also occur in viable cells and are therefore not

necessarily indicative of induction of cell death.<sup>28</sup> Importantly, though we did observe a time-dependent increase in annexin V binding, which was more pronounced for VHH1D17 than for the anti-CD1d mAb, this did not progress to actual cell death as the absolute number of living cells (ie, nuclear viability dye negative cells) was not affected. The intermediate annexin V binding levels on CD1d<sup>+</sup> tumor cells after VHH1D17 exposure further support absence of cell death as dying cells stained much brighter due to the massive PS externalization as a result of the collapsing cell membrane asymmetry. Indeed, it was suggested that both a critical concentration and topology of PS, as occurs in dying cells, is required for recognition as an "eat-me" signal for efferocytosis by macrophages.<sup>20</sup> The lack of engulfment of VHH1D17 exposed CD1d<sup>+</sup> tumor cells by moMacrophages thus underscores the absence of cell death induction.

Using anti-CD1d VHH1D22, which binds over the side of the F'-pocket of CD1d<sup>15</sup> (in contrast to VHH1D17 which binds over the A'-pocket of CD1d and leaves the lipid headgroup solvent exposed) and saposin KO cell lines, we demonstrated that the increase in annexin V binding to CD1d<sup>+</sup> tumor cells could be blocked by VHH1D22 and was critically dependent on saposins. These findings demonstrate saposin-mediated presentation of anionic phospholipid antigens by CD1d. Indeed, it has been shown that CD1d can present various anionic phospholipids known to bind annexin V.<sup>22</sup> It is known that annexin V can bind a range of anionic phospholipids<sup>17</sup> and we did not formally demonstrate which of these anionic phospholipid(s) were preferentially presented in CD1d as a result of VHH1D17 binding. Nevertheless, the subsequent ability of different TIM-molecules and bavituximab to bind, which have a reported specificity for PS and the PS-β2-GPI complex, respectively,<sup>27 29 30</sup> indicates that the most likely anionic phospholipid to be presented in CD1d is PS. Of note, since anti-CD1d mAbs block α-GalCer-CD1d mediated type 1 NKT cell activation,<sup>14</sup> the less pronounced increase in annexin V binding by the anti-CD1d mAb compared with VHH1D17 might be due to less effective saposin mediated PS-loading or steric hindrance of annexin V binding.

Despite highly similar folding of the VHH as well as docking to CD1d, VHH1D5 and VHH1D17 differ in their ability to enhance saposin-mediated PS loading in CD1d. This difference is likely explained by VHH1D17 Y59 and E108 that allowed for a conformational change in the CDR3 region that was specific to VHH1D17 and that led to the formation of an electrostatic negative patch at the VHH. As positively charged residues on the surface of saposins are considered important for their interaction with negatively charged membranes,<sup>31</sup> VHH1D17 could potentially facilitate CD1d-saposin interactions via this electrostatic negative patch and thereby affect lipid loading. If so, VHH1D17 would be another example of a CD1d-specific VHH that has intrinsic bispecificity (here by interacting with CD1d as well as saposins), as previously shown for anti-CD1d VHH1D12 that was found to



stabilize CD1d-type 1 NKT TCR interactions via intrinsic bispecificity.<sup>15</sup> Such preferential (saposin-mediated) loading of PS into CD1d might be further facilitated by the likely proximity of the CD1d-VHH1D17 complex and PS as it is known that CD1d localizes to caveolin-1 containing plasma membrane lipid rafts which can undergo caveolae-mediated endocytosis in a process that requires PS which is highly enriched in these vesicles.<sup>32–34</sup> Alternatively, though VHH1D17 did not appear to interfere with processing and presentation of  $\alpha$ -GalCer to type 1 NKT cells, the enhanced loading of PS could also result from interference of VHH1D17 with loading of other lipids.

In humans, the three different TIM family members (TIM-1, TIM-3 and TIM-4) that are known have all been recognized for their ability to bind PS and exert immunomodulatory functions.<sup>20–35</sup> TIM-3 in particular appears to play an important role as an immune checkpoint in autoimmunity and cancer and seems of particular importance for induction of antigen-specific tolerance.<sup>36</sup> Indeed, TIM-3 blockade is known to worsen disease in multiple preclinical autoimmune models, and patients harboring TIM-3 loss-of-function mutations exhibit a severe autoinflammatory and autoimmune phenotype.<sup>36</sup> We show that CD1d(PS) can interact with different human TIM-molecules and can induce TIM-3 signaling in a TIM-3 reporter cell assay, suggesting a functional CD1d(PS)-TIM-3-molecule axis. To the best of our knowledge, no such axis has been demonstrated to date. Earlier reports may have hinted in this direction as, for example, PS-loaded trophoblast CD1d might play a role in fetal tolerance,<sup>6–37</sup> and interleukin-10-producing regulatory B (B10) cells, a part of which expresses high levels of CD1d,<sup>38</sup> were significantly more often annexin V<sup>+</sup> than other B cells,<sup>39</sup> possibly reflecting PS-surface expression by CD1d. Although speculative, in light of these observations and our current results, it seems that the role of CD1d goes beyond providing direct lipid antigen-dependent TCR stimulation to CD1d-restricted T cells and can also provide co-stimulatory/inhibitory signals via ligation of TIM-molecules expressed on various immune cells. Future research is required to determine whether such CD1d(PS)-TIM interactions can indeed modulate immune responses and whether treatment with VHH1D17 could impact this. As PS binding proteins extend beyond annexin V,  $\beta$ 2-GP1, and TIM-molecules,<sup>40</sup> and lipids other than PS can be presented by CD1d,<sup>22</sup> future studies should explore whether other PS binding proteins are similarly impacted by VHH1D17 and whether other lipids presented by CD1d can modulate engagement of lipid binding proteins. Specifically, due to the ‘public’ conserved (monomorphic) nature of CD1d, it is likely that the effect of VHH1D17 would occur across the human population, and immune modulation might therefore be broadly applicable.

Collectively our data provide evidence that antibody targeting of CD1d using VHH1D17 (or anti-CD1d mAb

51.1) does not trigger cell death but enhances presentation of PS in CD1d which is accessible for (functional) interaction with therapeutic antibodies and immune regulatory TIM-molecules.

#### Author affiliations

<sup>1</sup>Department of Medical Oncology, Cancer Center Amsterdam, Amsterdam UMC Location VUmc, Amsterdam, The Netherlands

<sup>2</sup>Infection and Immunity Program and Department of Biochemistry and Molecular Biology, Biomedicine Discovery Institute, Monash University, Clayton, Victoria, Australia

<sup>3</sup>Department of Neurosurgery, Cancer Center Amsterdam, Amsterdam UMC Location VUmc, Amsterdam, The Netherlands

<sup>4</sup>Department of Microbiology and Immunology, Peter Doherty Institute for Infection and Immunity, The University of Melbourne, Melbourne, Victoria, Australia

<sup>5</sup>LAVA Therapeutics, Utrecht, The Netherlands

<sup>6</sup>Institute of Infection and Immunity, Cardiff University School of Medicine, Cardiff, UK

**Contributors** Conceptualization: RL, AS, DIG, JR, TDdG, HJvdV. Methodology: RL, AS, BW, DLH. Investigation: RL, AS, MV, BW, DLH, PB. Visualization: RL, AS, HJvdV. Resources: BW. Funding acquisition: DIG, JR, TDdG, HJvdV. Supervision: DIG, JR, TDdG, HJvdV. Writing original draft: RL, AS, TDdG, HJvdV. Guarantor: HJvdV

**Funding** This work was supported by CCA-VICI grant no. 2000483 from the VU University Medical Center, grant no. 140343 from Worldwide Cancer Research, funding from LAVA Therapeutics (RL, MV, DLH, PB and HJvdV), the National Health and Medical Research Council of Australia (NHMRC; grant nos. 1113293 and 1140126), and the Cancer Council of Victoria (JR and DIG). DIG was supported by an NHMRC Senior Principal Research Fellowship (no. 1117766) and subsequently by an NHMRC Investigator Award (2008913). JR is supported by an NHMRC Investigator award. AS is supported by an ARC DECRA Fellowship (DE210101031). We thank the Monash Macromolecular Crystallization Facility staff for assistance with crystallization, the Australian Synchrotron for assistance with data collection, the University of Melbourne, Department of Microbiology and Immunology Flow Cytometry facility for flow cytometry support, and Dr Adam P Uldrich for providing the SKW-3.NKT12 and SKW-3.NKT15 cells and the C1R.GFP cells expressing WT CD1d or mutant CD1d.

**Competing interests** DLH, PB and HJvdV are employees of LAVA Therapeutics, a company that develops bispecific gamma-delta T-cell engagers, and own LAVA Therapeutics shares and/or stock options. RL, TDdG and HJvdV are named inventors on international patent application WO 2016/122320 AI (‘Single domain antibodies targeting CD1d’) which partially relates to the work described in this paper. TDdG is a consultant for and a shareholder of LAVA Therapeutics. RL and MV were funded by a LAVA Therapeutics grant to Amsterdam UMC. JR has received funding from LAVA Therapeutics. DIG is a member of the scientific advisory board and a shareholder of Avalia Immunotherapies, a company working on NKT cell-based vaccines and is an inventor on patent applications WO 2021/127745 and WO 2021/127744 that describe effects of cross-linking CD1 molecules and WO2020/231274 that describes CD1d-dependent glycopeptide vaccines.

**Patient consent for publication** Not applicable.

**Ethics approval** Not applicable.

**Provenance and peer review** Not commissioned; externally peer reviewed.

**Data availability statement** Data are available in a public, open access repository. Data are available upon reasonable request. The crystal structure has been deposited in the Protein Data Bank, VHH1D17-hCD1d(sphingomyelin) (PDB accession code: 8SOS; DOI: <https://doi.org/10.2210/pdb8SOS/pdb>). All data reported in this paper will be shared by the lead contact upon request. This paper does not report original code. Any additional information required to reanalyze the data reported in this paper is available from the lead contact upon request.

**Supplemental material** This content has been supplied by the author(s). It has not been vetted by BMJ Publishing Group Limited (BMJ) and may not have been peer-reviewed. Any opinions or recommendations discussed are solely those of the author(s) and are not endorsed by BMJ. BMJ disclaims all liability and responsibility arising from any reliance placed on the content. Where the content includes any translated material, BMJ does not warrant the accuracy and reliability of the translations (including but not limited to local regulations, clinical guidelines,

terminology, drug names and drug dosages), and is not responsible for any error and/or omissions arising from translation and adaptation or otherwise.

**Open access** This is an open access article distributed in accordance with the Creative Commons Attribution Non Commercial (CC BY-NC 4.0) license, which permits others to distribute, remix, adapt, build upon this work non-commercially, and license their derivative works on different terms, provided the original work is properly cited, appropriate credit is given, any changes made indicated, and the use is non-commercial. See <http://creativecommons.org/licenses/by-nc/4.0/>.

#### ORCID iD

Roeland Lameris <http://orcid.org/0000-0003-4729-8863>

#### REFERENCES

- Chancellor A, Gadola SD, Mansour S. The versatility of the CD1 lipid antigen presentation pathway. *Immunology* 2018;154:196–203.
- Moody DB, Cotton RN. Four pathways of CD1 antigen presentation to T cells. *Curr Opin Immunol* 2017;46:127–33.
- Nair S, Dhodapkar MV. Natural killer T cells in cancer immunotherapy. *Front Immunol* 2017;8:1178.
- McEwen-Smith RM, Salio M, Cerundolo V. The regulatory role of invariant NKT cells in tumor immunity. *Cancer Immunol Res* 2015;3:425–35.
- de Weerd I, Lameris R, Ruben JM, et al. A Bispecific single-domain antibody boosts autologous Vγ9Vδ2-T cell responses toward CD1d in chronic lymphocytic leukemia. *Clin Cancer Res* 2021;27:1744–55.
- Iwasawa Y, Kawana K, Fujii T, et al. A possible coagulation-independent mechanism for pregnancy loss involving β(2) glycoprotein 1-dependent antiphospholipid antibodies and CD1d. *Am J Reprod Immunol* 2012;67:54–65.
- Colgan SP, Hershsberg RM, Furuta GT, et al. Ligation of intestinal epithelial CD1d induces bioactive IL-10: critical role of the cytoplasmic tail in autocrine signaling. *Proc Natl Acad Sci U S A* 1999;96:13938–43.
- Teyton L. Role of lipid transfer proteins in loading CD1 antigen-presenting molecules. *J Lipid Res* 2018;59:1367–73.
- Godfrey DI, Le Nours J, Andrews DM, et al. Unconventional T cell targets for cancer immunotherapy. *Immunity* 2018;48:453–73.
- Exley MA, Tahir SM, Cheng O, et al. A major fraction of human bone marrow lymphocytes are Th2-like CD1d-reactive T cells that can suppress mixed lymphocyte responses. *J Immunol* 2001;167:5531–4.
- Yue SC, Shaulov A, Wang R, et al. CD1d ligation on human monocytes directly signals rapid NF-κappaB activation and production of bioactive IL-12. *Proc Natl Acad Sci U S A* 2005;102:11811–6.
- Spanoudakis E, Hu M, Naresh K, et al. Regulation of multiple myeloma survival and progression by CD1d. *Blood* 2009;113:2498–507.
- Theodorou ID, Bounsell L, Calvo CF, et al. CD1 stimulation of human T cell lines induces a rapid increase in the intracellular free Ca<sup>2+</sup> concentration and the production of IL-2. *J Immunol* 1990;144:2518–23.
- Lameris R, de Bruin RCG, van Bergen En Henegouwen PMP, et al. Generation and characterization of CD1d-specific single-domain antibodies with distinct functional features. *Immunology* 2016;149:111–21.
- Lameris R, Shahine A, Pellicci DG, et al. A single-domain bispecific antibody targeting CD1d and the NKT T-cell receptor induces a potent antitumor response. *Nat Cancer* 2020;1:1054–65.
- Ran FA, Hsu PD, Wright J, et al. Genome engineering using the CRISPR-Cas9 system. *Nat Protoc* 2013;8:2281–308.
- Maffey KG, Keil LB, DeBari VA. The influence of lipid composition and divalent cations on annexin V binding to phospholipid mixtures. *Ann Clin Lab Sci* 2001;31:85–90.
- Kang SJ, Cresswell P. Regulation of intracellular trafficking of human CD1d by association with MHC class II molecules. *EMBO J* 2002;21:1650–60.
- Chen X, Wang X, Keaton JM, et al. Distinct endosomal trafficking requirements for presentation of autoantigens and exogenous lipids by human CD1d molecules. *J Immunol* 2007;178:6181–90.
- Birge RB, Boeltz S, Kumar S, et al. Phosphatidylserine is a global immunosuppressive signal in efferocytosis, infectious disease, and cancer. *Cell Death Differ* 2016;23:962–78.
- Fischer K, Voelkl S, Berger J, et al. Antigen recognition induces phosphatidylserine exposure on the cell surface of human CD8+ T cells. *Blood* 2006;108:4094–101.
- Cox D, Fox L, Tian R, et al. Determination of cellular lipids bound to human CD1d molecules. *PLoS One* 2009;4:e5325.
- Borg NA, Wun KS, Kjer-Nielsen L, et al. CD1d-lipid-antigen recognition by the semi-invariant NKT T-cell receptor. *Nature* 2007;448:44–9.
- Jurus E, Engel D, Star K, et al. Improvements to the APBS biomolecular solvation software suite. *Protein Sci* 2018;27:112–28.
- Ohkuma S, Poole B. Fluorescence probe measurement of the intralysosomal pH in living cells and the perturbation of pH by various agents. *Proc Natl Acad Sci U S A* 1978;75:3327–31.
- Lemke G. How macrophages deal with death. *Nat Rev Immunol* 2019;19:539–49.
- Luster TA, He J, Huang X, et al. Plasma protein beta-2-glycoprotein 1 mediates interaction between the anti-tumor monoclonal antibody 3G4 and anionic phospholipids on endothelial cells. *J Biol Chem* 2006;281:29863–71.
- Kepp O, Galluzzi L, Lipinski M, et al. Cell death assays for drug discovery. *Nat Rev Drug Discov* 2011;10:221–37.
- Kobayashi N, Karisola P, Peña-Cruz V, et al. TIM-1 and TIM-4 glycoproteins bind phosphatidylserine and mediate uptake of apoptotic cells. *Immunity* 2007;27:927–40.
- Smith CM, Li A, Krishnamurthy N, et al. Phosphatidylserine binding directly regulates TIM-3 function. *Biochem J* 2021;478:3331–49.
- Rossmann M, Schultz-Heienbrock R, Behlke J, et al. Crystal structures of human saposins C and D: implications for lipid recognition and membrane interactions. *Structure* 2008;16:809–17.
- Nowyhed HN, Chandra S, Kiosses W, et al. ATP binding cassette transporter ABCA7 regulates NKT cell development and function by controlling CD1d expression and lipid raft content. *Sci Rep* 2017;7:40273.
- Kiss AL, Botos E. Endocytosis via caveolae: alternative pathway with distinct cellular compartments to avoid lysosomal degradation. *J Cell Mol Med* 2009;13:1228–37.
- Fairn GD, Schieber NL, Ariotti N, et al. High-resolution mapping reveals topologically distinct cellular pools of phosphatidylserine. *J Cell Biol* 2011;194:257–75.
- Sabatós-Peyton CA, Nevin J, Brock A, et al. Blockade of Tim-3 binding to phosphatidylserine and ceacam1 is a shared feature of anti-Tim-3 antibodies that have functional efficacy. *Oncoimmunology* 2018;7:e1385690.
- Wolf Y, Anderson AC, Kuchroo VK. TIM3 comes of age as an inhibitory receptor. *Nat Rev Immunol* 2020;20:173–85.
- Wang S-C, Li Y-H, Piao H-L, et al. PD-1 and Tim-3 pathways are associated with regulatory CD8+ T-cell function in decidua and maintenance of normal pregnancy. *Cell Death Dis* 2015;6:e1738.
- Zeng SG, Ghnewa YG, O'Reilly VP, et al. Human invariant NKT cell subsets differentially promote differentiation, antibody production, and T cell stimulation by B cells in vitro. *J Immunol* 2013;191:1666–76.
- Audo R, Hua C, Hahne M, et al. Phosphatidylserine outer layer translocation is implicated in IL-10 secretion by human regulatory B cells. *PLoS One* 2017;12:e0169755.
- Naeini MB, Bianconi V, Pirro M, et al. The role of phosphatidylserine recognition receptors in multiple biological functions. *Cell Mol Biol Lett* 2020;25:23.